Modeling and Analysis of Handover Failure Probability in Small Cell Networks

Carlos H. M. de Lima, Mehdi Bennis and Matti Latva-aho
Centre for Wireless Communications
University of Oulu
P. O. Box 4500, FIN-90014
Email: {carlosl, bennis, matla}@ee.oulu.fi

***Abstract*—Mobility management in small cell networks is of utmost importance, and is currently under study in 3GPP Release–12. In this article, we model and analyze the outbound handover failure probability in small cell networks, in which a given user crosses its serving cell coverage border before his time-to-trigger elapses, without connecting to his target base station. Using tools from stochastic geometry, a closed-form expression of the handover link failure probability is characterized, as a function of shadowed channel fading, hysteresis margin, time-to-trigger, users' velocity and traveled distances. Numerical results show the effectiveness of the proposed analytical model and provide key insights into the problem of mobility management.**

I. Introduction

In classical wireless cellular networks, User Equipments (UEs) are handed over when the signal quality of the target cell is higher than the source cell plus a hysteresis margin, and during a Time-To-Trigger (TTT) duration. The underlying assumption of the Handover (HO) procedure in macrocellular networks is that all UEs use the same hysteresis margin and TTT values. However, using the same HO parameters in Heterogeneous Networks (HetNets) may severely degrade the network performance as the probability of having high-speed UEs under the coverage of small cell Base Stations (BSs) increases incurring HO failures.

Recently, mobility management in HetNets received significant attention from both industry and academia [1]–[4]. In [1], a coordination-based mechanism is proposed, whereby picocells mute their transmissions on certain time slots not to interfere with high-speed UEs. In [2], the authors evaluate the performance of mobility management in LTE-Advanced systems using Carrier Aggregation (CA), in which mobile UEs autonomously add small cells for hotspot coverage. In [3], mobility enhancements based on UE mobility state estimation are proposed, in which high-speed UEs are kept at the macro layer, while low-speed UEs are handed over to picocells. In [4], the authors provide closed-form expressions for the HO failure and ping-pong probabilities, as a function of the TTT, UE velocity and traveled distance. Beyond [4], the vast majority of these works require time-consuming Monte-Carlo simulations, and fall short of providing insights into the fundamental challenges of mobility management in HetNets.

In this article, we investigate the problem of mobility management in small cell networks by providing a closed-form expression of the outbound handover failure probability, as a function of the channel fading, velocity, TTT and users' traveled distance. We focus on the scenario in which a typical pico UE is traversing his serving Pico-BS, at a given velocity, and is handed over to his next target cell. As in [4], we assume that the picocell coverage and radio link failure areas are modeled as circles, and the users' trajectories are linear. Leveraging the developed mobility model we analyze the impact of the HO parameters (i.e., users' velocities, TTT and users' traveled distance) on the network performance.

This paper is organized as follows. Section II presents the considered system model. Section III examines the mobility control and handover failure aspects. Numerical results are shown in Section IV and conclusions drawn in Section V.

II. System Model

We study the Downlink (DL) of a multi-tier deployment scenario in which small cells coexist with the legacy macrocellular network. BSs operate in Time Division Duplexing (TDD) mode and independently schedule a random UE at every transmission time interval. Communicating nodes use antennas with omni directional radiation pattern. Radio links are affected by path-loss, large-scale shadowing and multi-path fading assumed to be mutually independent and multiplicative phenomena [5], [6]. The received power at the user of

978-1-4799-3088-3/14/$31.00 ©2014 IEEE

interest from an arbitrary transmitter located r meters away is given by:

$$Y = p\, r^{-\alpha} x, \tag{1}$$

where p is the downlink BS transmit power, α is the path-loss exponent and x represents the shadowed fading channel.

The composite squared envelop due to Log-Normal (LN) shadowing and Nakagami-m fading is represented by a Random Variable (RV), $X \in \mathbb{R}^+$, with Probability Density Function (PDF) $f_X(x)$, which follows a Gamma-LN distribution. A single LN distribution with mean and standard deviation given by:

$$\begin{aligned} \mu_{\mathrm{dB}} &= \xi\left[\psi(m) - \ln(m)\right] + \mu_{\Omega_p}, \\ \sigma^2_{\mathrm{dB}} &= \xi^2 \zeta(2, m) + \sigma^2_{\Omega_p}, \end{aligned} \tag{2}$$

is used to approximate the Gamma-LN distribution [7], where $\psi(\cdot)$ is the Euler psi function and $\zeta(2,\cdot)$ is the generalized Riemann zeta function [8], m is the shape parameter of the Gamma distribution, $\xi = \ln(10)/10$, and Ω_p is a RV representing the mean squared-envelope whose mean and standard deviation are given by μ_{Ω_p} and σ_{Ω_p}, respectively.

Spatial Poisson Point Processes (PPPs) Φ^{BS} (Φ^{UE}) represent the locations of BSs (UEs), respectively. The shadowed fading is associated as a random mark to each point of the above processes [9] and is assumed to be independent over distinct network entities and positions. By virtue of the Marking theorem [10], the resulting processes constitute Marked Point Processes (MPPs) on the product space $\mathbb{R}^2 \times \mathbb{R}^+$, whose random points φ^{BS} (φ^{UE}) denote the locations of BSs (UEs), namely:

$$\begin{aligned} \widetilde{\Phi}^{\mathsf{BS}} &= \left\{(\varphi, x)\,;\, \varphi \in \Phi^{\mathsf{BS}}\right\}, \\ \widetilde{\Phi}^{\mathsf{UE}} &= \left\{(\varphi, x)\,;\, \varphi \in \Phi^{\mathsf{UE}}\right\}. \end{aligned} \tag{3}$$

Note that $\widetilde{\Phi}^{\mathsf{BS}}$ and $\widetilde{\Phi}^{\mathsf{BS}}$ are assumed to be independent spatial PPPs.

To carry out our investigations, an annular observation region $\mathcal{O}$, which is delimited by the minimum and maximum radii R_m and R_M, respectively, is defined around the tagged receiver (*i.e.*, UE of interest). The random trajectory of the ith UE is characterized by the following tuple:

$$\mathsf{T}_i = \left(\varphi_i^{\mathsf{UE}}, \theta_i, v_i\right), \tag{4}$$

where $\varphi_i^{\mathsf{UE}} \in \Phi^{\mathsf{UE}}$ yields the initial location of the ith user within the coverage of its serving BS, $\theta_i \in [0, 2\pi]$ is a random orientation and v_i is the ith user's velocity.

Fig. 1 illustrates random trajectories of UEs within the coverage of an arbitrary BS. In this figure the inner circle corresponds to the handover triggering region with circumference in solid line, while the outer circle gives the coverage region with circumference in dashed line. In the following, the mobility control procedure is characterized in terms of its configuration parameters, namely, TTT and handover hysteresis margin Ω, as well as the handover triggering and coverage regions as indicated in Fig. 1.

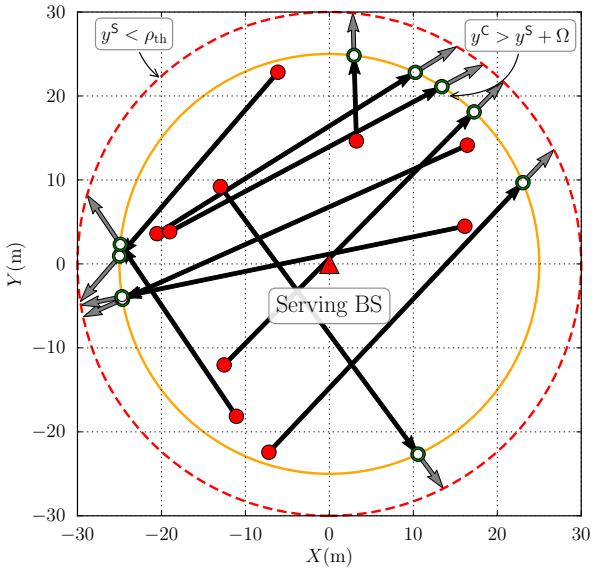

Fig. 1. Random trajectories of UEs within the coverage of an arbitrary BS. Inner and outer circles define the handover triggering and coverage regions, respectively.

III. Mobility Control and Handover Failure Probability

We follow the standard handover procedure as defined in the 3GPP specifications [11], in which the handover procedure is initiated (triggering event) when the received signal strength of the candidate/target BS exceeds that of the serving BS, by a hysteresis margin:

$$\Upsilon_{\mathsf{ho}} = \left\{Y^{\mathsf{C}} > Y^{\mathsf{S}} + \Omega\right\}, \tag{5}$$

where Y^{C} and Y^{S} are RVs representing the received power, at the user of interest, from the candidate and serving BS, respectively and Ω is the handover hysteresis margin.

For a radio channel affected by Nakagami-m fading and LN shadowing, the Characteristic Function (CF) and cumulants of the received power at the tagged receiver from a random transmitter inside the observation region $\mathcal{O}$ are defined in [12]. Using the aforesaid results, (5) and the LN approximation in (2), we derive the probability that the event Υ_{ho} occurs as follows.

Proposition 1: Consider the observation region $\mathcal{O}$ centered at the tagged receiver and the standard handover procedure as described above. Then, the probabil-

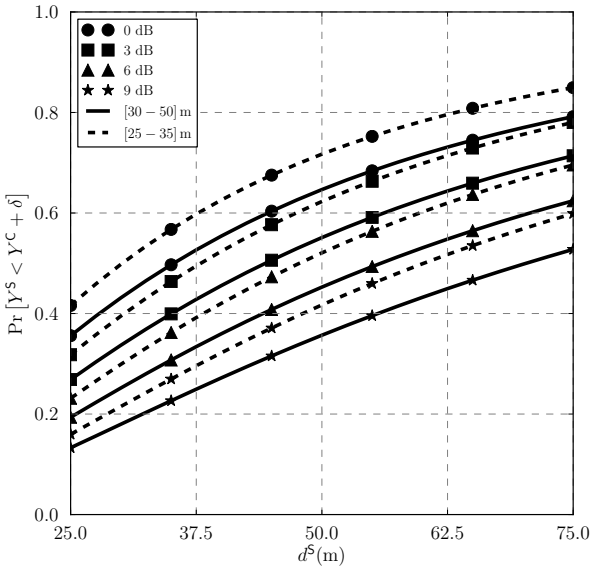

Fig. 2. Probability that the event Υ_{ho} occurs for distinct network configurations: channel parameters, d^{S}, Ω. In the legends, $[R_m - R_M]$ indicates the minimum and maximum distance to the random candidate BS from the user of interest.

ity that the handover event is triggered when the serving BS is located d^{S} meters away and the candidate BS is randomly deployed in $\mathcal{O}$ is:

$$\Pr\left[Y^{\mathsf{S}} < Y^{\mathsf{C}} + \delta\right] \simeq \sum_{k=1}^{K} \frac{\omega_k}{2\sqrt{\pi}} g\left(\eta_k\right), \tag{6}$$

where $\delta = -\Omega$, η_k is the kth zero of the Hermite polynomial $H_K\left(\eta\right)$ of degree K, ω_k is the corresponding weight of the function $g\left(\cdot\right)$ at the kth abscissa and $g\left(\eta\right) = 1 + \mathrm{Erf}\left[\frac{-\mu_S + \mu_C + \sqrt{2}\eta\sigma_C}{\sqrt{2}\sigma_S}\right]$.

Proof: See Appendix A. ■

Fig. 2 shows how the handover probability varies with distinct network configurations, namely the UE traveled distance from its serving BS (d^S) and various hysteresis margin values (Ω). As can be seen, the triggering handover probability increases as the UE traverses its own serving cell. In addition, the triggering HO probability decreases with increasing hysteresis margin values.

A. Coverage and Handover Radii Estimation

The handover procedure fails if the user of interest is not handed over to the candidate BS before it reaches its serving cell coverage border, *i.e.*, $Y^{\mathsf{S}} < \rho_{\mathrm{th}}$. In order to properly characterize the handover failure probability, the radii R_h and R_c defining the handover triggering and coverage regions, need to be estimated. Thereafter, the time needed to trigger the handover TTT is compared against the time traveled by the user of interest within the annular region delimited by R_h and R_c.

First, the coverage region of an arbitrary BS is determined as a function of the network configuration and radio channel impairments. The coverage radius R_c (cell edge border) is defined to guarantee a target coverage reliability which is ensured with an arbitrary fade margin FM [13].

Lemma 1: Consider the network and composite shadowed fading models of Section II; then, the cell edge reliability is given by:

$$\Pr\left[pR_c^{-\alpha}x \geqslant \rho_{\mathrm{th}}\right] = 1 - \mathrm{Q}\left[\mathsf{FM}/\sigma\right] \tag{7}$$

where $\mathsf{FM} = \rho_{\mathrm{th}} - \mu$ yields the fade margin and $\mathrm{Q}[u] = \frac{1}{\sqrt{2\pi}}\int_u^\infty e^{-\frac{v^2}{2}}\,\mathrm{d}v$.

Using Lemma 1, the useful service area is determined such that within the circular coverage region of radius R_c the received signal strength exceeds the detection threshold ρ_{th} [14]. Similar to (5), the event of the UE being covered is mathematically described by the following event:

$$\Upsilon_{\mathsf{cv}} = \left\{pr^{-\alpha}x \geqslant \rho_{\mathrm{th}}\right\}. \tag{8}$$

Similarly, (5) is used to determine the handover triggering radius R_h and set the handover target probability.

B. Handover Failure Probability

Following this formulation, the handover procedure fails if the user of interest crosses its serving cell coverage border before the TTT elapses and without connecting to the candidate BS. In other words, the received signal strength drops below the detection threshold and the connection is lost. To derive the handover failure probability, we need to first characterize the distribution of the handover triggering distance denoted by D. In Fig. 3, an arbitrary trajectory $\mathsf{T} = \left(\varphi^{\mathsf{UE}}, \theta, v\right)$ is used to compute relevant metrics and characterize the mobility profile of UEs. To begin with, the distribution of the aperture angle $\widehat{\mathrm{COC}'}$ denoted by θ (see Fig. 3) is derived.

Lemma 2: Consider the trajectory $\left(\varphi^{\mathsf{UE}}, \theta, v\right)$ of the user of interest; then, the distribution of the aperture angle θ is given by:

$$F_\Theta\left(\theta\right) = \frac{\left(2\pi - \theta\right)\theta}{\pi^2}, 0 \leqslant \theta \leqslant 2\pi. \tag{9}$$

where Θ is a RV representing the aperture angle as indicated in Fig. 3.

Proof: See Appendix B ■

Next, the direction angle $\widehat{\mathrm{CHH}'}$ denoted by β is derived using Lemma 2 as follows.

Lemma 3: Consider the UE trajectory defined by the tuple $\left(\varphi^{\mathsf{UE}}, \theta, v\right)$; then, the distribution of the orientation

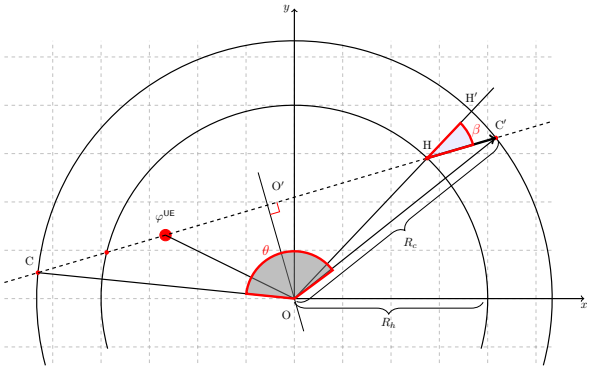

Fig. 3. Illustration of a given user trajectory characterized by the tuple $(\varphi^{\mathsf{UE}}, \theta, v)$, along its serving cell.

angle β is given by:

$$F_B(\beta) = 1 - F_\Theta\left(2\arccos\left[\frac{R_h}{R_c}\sin\beta\right]\right), \qquad (10)$$

where R_h and R_c yield the handover and coverage radii, respectively.

Proof: See Appendix C ■

The probability distribution of the distance traveled by the tagged receiver, denoted by D, along its trajectory $(\varphi^{\mathsf{UE}}, \theta, v)$ and between the handover triggering and coverage regions is derived next.

Theorem 1: Consider the handover procedure as described in Section III. Then, the PDF of the distance D is given in (11), where R_c is the coverage region radius, R_h is the handover triggering region radius and d is the distance traveled during the handover procedure.

Proof: See Appendix D. ■

The handover failure probability $\mathsf{P}_{\mathsf{fail}}$ corresponds to the probability that the tagged UE moves past the coverage region of its serving BS before the handover procedure is successful during the TTT duration, and fails to connect to the target BS.

Theorem 2: Consider the handover procedure of Section III; then, the probability of handover failure is given by:

$$\mathsf{P}_{\mathsf{fail}} = \Pr\left[D < v\Delta T\right] \qquad (12)$$

where ΔT is a network parameter.

Proof: In accordance with the system model in Section II, the user of interest travels at a constant velocity v. The distance traveled by the user of interest during the TTT is given by $\Delta d = v\Delta T$. In order to successfully complete the handover procedure, the user of interest needs to switch to the candidate BS before the received signal strength from its serving BS drops below the detection level as indicated in (8). ■

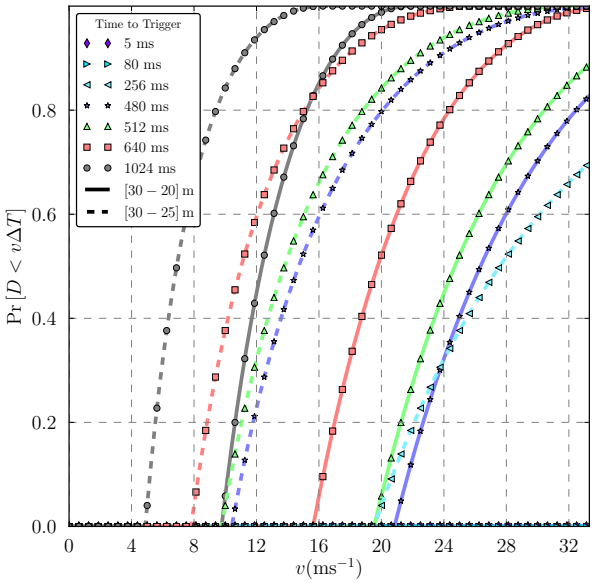

Fig. 4. Probability of handover failure as a function of users' velocities and TTT values.

IV. Numerical Results

In this section, we evaluate how the mobility control procedure works under various network configurations, radio channel conditions and user mobility profiles. The probability of handover failure $\mathsf{P}_{\mathsf{fail}}$ (see Section III) is used to assess the performance of the handover procedure.

Fig. 4 shows the probability of handover failure for increasing mobile velocity values v and varying TTT as specified in [15]. To set the handover triggering and coverage regions, we consider a shadowed fading channel with Nakagami-m shape parameter $m = 16$, LN shadowing standard deviation $\sigma = 8\,\mathrm{dB}$ and path-loss exponent $\alpha = 3$. In addition, the serving BS transmit power is $20\,\mathrm{dBm}$ and the handover hysteresis margin is $\Omega = 3\,\mathrm{dB}$. In this plot, we evaluate $\Pr\left[D < v\Delta T\right]$ that is the probability that the distance traveled by the user of interest with constant velocity v after triggering the handover procedure is not larger than the handover distance. Specifically, with a handover threshold of $\rho_{\mathsf{ho}} = -17\,\mathrm{dBm}$, the handover radius is $R_{\mathrm{h}} = 16.73\,\mathrm{m}$, while for $\rho_{\mathsf{min}} = -26\,\mathrm{dBm}$, $R_{\mathrm{c}} = 33.38\,\mathrm{m}$, which guarantees a cell edge and coverage area reliability of about $90\,\%$ and $99\,\%$, respectively. In addition, the handover traveling distance depends not only on the channel impairments, but also on the predefined detection and handover triggering thresholds.

In traditional cellular systems, a longer TTT prevents

$$f_D(d) = \frac{2\left(d^2 - R_c^2 + R_h^2\right)\left(-\frac{-d^2+R_c^2-R_h^2}{2d^2R_h} - \frac{1}{R_h}\right)\arcsin\left(\frac{R_h\sqrt{1-\frac{\left(d^2-R_c^2+R_h^2\right)^2}{4d^2R_h^2}}}{R_c}\right)}{dR_c\sqrt{\frac{\left(d^2+R_c^2-R_h^2\right)^2}{d^2R_c^2}}\sqrt{1-\frac{\left(-d^2+R_c^2-R_h^2\right)^2}{4d^2R_h^2}}\arcsin\left(\frac{R_h}{R_c}\right)^2} \tag{11}$$

UEs from switching back and forth between adjacent BSs (a.k.a ping-pong effect). Conversely, if the TTT is too short the user of interest may react too soon to a momentary channel variation and then be exposed to a ping-pong effect. In highly dense deployment scenarios with short range small cells, the probability of handover failure decreases with shorter TTT as evidenced by Fig. 4. For instance, the handover failure probability is about $85\,\%$ with $1024\,\text{ms}$ TTT, while it becomes approximately $5\,\%$ with $640\,\text{ms}$. In addition, as Fig. 4 shows, the handover failure probability also increases for longer handover triggering regions. The aforementioned effect happens by considering higher handover hysteresis margin values and pushing the handover triggering region closer to the cell's coverage border.

V. Conclusions

In this paper, we studied the problem of mobility management in small cell networks by providing a closed-form expression of the outbound handover failure probability, as a function of various network parameters. It was shown that the handover failure probability increases for longer TTT values as the UEs get closer to the cell's coverage border before their TTT expires. Future work will leverage the proposed analytical model in a multi-tier setting so as to optimize cell-specific handover parameters as a function of the traffic load, intercell and interference coordination, and users' mobility patterns. Besides, we will characterize the inherent tradeoffs between handover failure probability and ping-pong.

Appendix A
Proof of Proposition 1

From (2), Y^{C} and Y^{S} follow LN distribution with parameters $(\mu_{\mathrm{S}}, \sigma_{\mathrm{S}})$ and $(\mu_{\mathrm{C}}, \sigma_{\mathrm{C}})$, respectively. The handover probability P_{ho} is given by

$$\begin{aligned}\mathsf{P}_{\mathrm{ho}} &= \Pr\left[Y^{\mathrm{S}} < Y^{\mathrm{C}} + \delta\right] \\ &= \int_0^{\infty}\int_0^{y^{\mathrm{C}}+c} f_{Y^{\mathrm{S}}}\left(y^{\mathrm{S}}\right) f_{Y^{\mathsf{C}}}\left(y^{\mathrm{C}}\right) \mathrm{d}y^{\mathrm{S}}\mathrm{d}y^{\mathrm{C}}. \end{aligned} \tag{13}$$

where $f_{Y^{\mathrm{S}}}\left(y^{\mathsf{S}}\right)$ and $f_{Y^{\mathsf{C}}}\left(y^{\mathsf{C}}\right)$ yield the probability density function of the serving and candidate BSs, respectively. After evaluating the inner-most integral with respect to y^{S}, we obtain

$$\mathsf{P}_{\mathsf{ho}} = \int_0^{\infty} \frac{1}{2}\,\mathrm{Erfc}\left[\frac{\mu_{\mathsf{S}} - \log\left(c + y^{\mathsf{C}}\right)}{\sqrt{2}\sigma_{\mathsf{S}}}\right] f_{Y^{\mathsf{C}}}\left(y^{\mathsf{C}}\right) \mathrm{d}y^{\mathsf{C}}. \tag{14}$$

After making the change of variate $\eta = \frac{-\mu_{\mathsf{C}} + \log\left(y^{\mathsf{C}}\right)}{\sqrt{2}\sigma_{\mathsf{C}}}$ in (14), we obtain

$$\mathsf{P}_{\mathrm{ho}} = \int_{-\infty}^{\infty} \frac{e^{-\eta^2}\,\mathrm{Erfc}\left[\frac{\mu_{\mathsf{S}} - \log\left(c + e^{\mu_{\mathsf{C}} + \sqrt{2}\eta\sigma_{\mathsf{C}}}\right)}{\sqrt{2}\sigma_{\mathsf{S}}}\right]}{2\sqrt{\pi}} \mathrm{d}\eta. \tag{15}$$

Gauss-Hermite quadrature is then used to evaluate $\Pr\left[Y^{\mathsf{S}} < Y^{\mathsf{C}} + \delta\right]$ in (15) [8],

$$\int_{-\infty}^{+\infty} e^{-\eta^2} f(\eta)\, d\eta = \sum_{k=1}^{K} \omega_k f\left(\eta_k\right) + R_K, \tag{16}$$

where η_k is the kth zero of the Hermite polynomial $H_K(\eta)$ of degree K, ω_k is the corresponding weight of the function $f(\cdot)$ at the kth abscissa, and R_K is the remainder value. Finally, we obtain (6) by performing the substitutions indicated above.

Appendix B
Proof of Lemma 2

From Fig 3, the aperture angle θ is formed by the intersections points between the trajectory of the tagged user and coverage circle. Without loss of generality, the upper half of the coverage circle is considered to compute the distribution of Θ as follows [16],

$$\begin{aligned} F_{\Theta}(\theta) &= \int\int_{\mathcal{S}} f_{\theta_i,\theta_0}(\theta_i,\theta_0)\,\mathrm{d}\theta_i\mathrm{d}\theta_0 \\ &= \int_0^{\theta}\int_0^{\theta+\theta_i} \mathrm{d}\theta_0\,\mathrm{d}\theta_i + \int_{\pi-\theta}^{\pi}\int_{\theta_i-\theta}^{\pi} \mathrm{d}\theta_0\,\mathrm{d}\theta_i \qquad (17) \\ &\quad + \int_{\theta}^{\pi-\theta}\int_{\theta_i-\theta}^{\theta+\theta_i} \mathrm{d}\theta_0\,\mathrm{d}\theta_i/\pi^2 \qquad (18) \\ &= \frac{(2\pi-\theta)\,\theta}{\pi^2}, 0 \leqslant \theta \leqslant \pi. \qquad (19) \end{aligned}$$

where $f_{\theta_i,\theta_0}(\theta_i,\theta_0)$ is the joint distribution of the angles θ_a and θ_b.

By taking the derivative of (19), the PDF of the aperture angle θ is obtained in (9).

Appendix C
Proof of Lemma 3

As shown in [17], the orientation angle β within the interval $[-\pi/2, \pi/2]$. Without lack of generality, we consider β within the interval $[0, \pi/2]$

$$c = \int_0^{2\arccos(R_h/R_c)} f_\Theta(\theta)\,\mathrm{d}\theta \tag{20}$$

$$\begin{aligned}
\Pr[B \leqslant \beta] &= \Pr\left\{\arcsin\left[\frac{R_c}{R_h}\cos(\theta/2)\right] \leqslant \beta\right\} \\
&= \Pr\left[\cos(\theta/2) \leqslant \frac{R_h}{R_c}\sin\beta\right] \\
&\overset{(a)}{=} \Pr\left\{\theta \geqslant 2\arccos\left[\frac{R_h}{R_c}\sin\beta\right]\right\} \\
F_B(\beta) &= 1 - F_\Theta\left(2\arccos\left[\frac{R_h}{R_c}\sin\beta\right]\right) \\
f_B(\beta) &\overset{(b)}{=} -f_\Theta\left(2\arccos\left[\frac{R_h}{R_c}\sin\beta\right]\right) \\
&\quad \times \frac{\partial}{\partial\beta}\left(2\arccos\left[\frac{R_h}{R_c}\sin\beta\right]\right)
\end{aligned} \tag{21}$$

where (a) is obtained since the arccosine function is monotonically decreasing, (b) is obtained by taking the first-order derivative of $F_B(\beta)$.

Appendix D
Proof of Theorem 1

We derive the probability distribution function of the handover dwelling distance by using Lemmas 1 and 2, as well as the standard procedure to derive the distribution of a function of a single random variable $D = g(\beta)$. From the right triangle $\widehat{\mathrm{OO'C'}}$, we can write that:

$$\begin{aligned}
(D + R_h\cos\beta)^2 &= R_c^2 - (R_h\sin\beta)^2 \\
\Pr[D < d] &= \Pr\left[\beta < \arccos\left(\frac{R_c^2 - R_h^2 - d^2}{2\,d\,R_h}\right)\right]
\end{aligned} \tag{22}$$

Then, using the same procedure to derive Lemma 2 and assuming that the distance is positive, we obtain:

$$F_D(d) = F_B\left[\arccos\left(\frac{R_c^2 - R_h^2 - d^2}{2\,d\,R_h}\right)\right] \tag{23}$$

$$\begin{aligned}
f_D(d) &= f_B\left[\arccos\left(\frac{R_c^2 - R_h^2 - d^2}{2\,d\,R_h}\right)\right] \\
&\quad \times \frac{\partial}{\partial d}\arccos\left(\frac{R_c^2 - R_h^2 - d^2}{2\,d\,R_h}\right)
\end{aligned} \tag{24}$$

Acknowledgements

This work is supported by the SHARING project under the Finland grant 128010. The authors would like to thank the Brazilian Science without Boarders Special Visiting Researcher fellowship CAPES 076/2012.

References

[1] D. López-Pérez, I. Güvenç, and X. Chu, "Mobility management challenges in 3gpp heterogeneous networks," *IEEE Communications Magazine*, vol. 50, no. 12, pp. 70–78, 2012.

[2] K. Pedersen, P. Michaelsen, C. Rosa, and S. Barbera, "Mobility enhancements for lte-advanced multilayer networks with inter-site carrier aggregation," *Communications Magazine, IEEE*, vol. 51, no. 5, pp. –, 2013.

[3] P. Munoz, R. Barco, D. Laselva, and P. Mogensen, "Mobility-based strategies for traffic steering in heterogeneous networks," *Communications Magazine, IEEE*, vol. 51, no. 5, pp. –, 2013.

[4] D. López-Pérez, I. Güvenç, and X. Chu, "Theoretical analysis of handover failure and ping-pong rates for heterogeneous networks," in *ICC*, 2012, pp. 6774–6779.

[5] J. Ilow and D. Hatzinakos, "Analytic alpha-stable noise modeling in a poisson field of interferers or scatterers," *IEEE Trans. Signal Process.*, vol. 46, no. 6, pp. 1601–1611, Jun. 1998.

[6] M.-S. Alouini and A. J. Goldsmith, "Area spectral efficiency of cellular mobile radio systems," *IEEE Trans. Wireless Commun.*, vol. 48, no. 4, pp. 1047–1066, Jul. 1999.

[7] M.-J. Ho and G. L. Stüber, "Capacity and power control for CDMA microcells," *ACM Journal on Wireless Networks*, vol. 1, no. 3, pp. 355–363, Oct. 1995.

[8] M. Abramowitz and I. A. Stegun, *Handbook of Mathematical Functions with Formulas, Graphs, and Mathematical Tables*, 9th ed. Dover, 1965.

[9] A. Ghasemi and E. S. Sousa, "Interference aggregation in spectrum-sensing cognitive wireless networks," *IEEE J. Sel. Areas Commun.*, vol. 2, no. 1, pp. 41–56, Feb. 2008.

[10] J. F. C. Kingman, *Poisson Processes*. Oxford University Press, 1993.

[11] 3GPP, "3G home Node B study item," TS23.009, version 11.0.0 release 11, Tech. Rep., Sep. 2011.

[12] C. H. M. de Lima, M. Bennis, and M. Latva-aho, "Statistical analysis of self-organizing heterogeneous networks with biased cell association and interference avoidance," *IEEE Trans. Veh. Technol.*, vol. 62, no. 6, Special Issue on Self-Organizing Radio Networks 2013.

[13] W. C. Jakes, Ed., *Microwave mobile communications*, 2nd ed. Wiley-IEEE Press, 1994.

[14] T. S. Rappaport, *Wireless Communications: Principles and Practice*, 2nd ed. Prentice Hall, 2002.

[15] 3GPP, "RRC protocol specification," TS36.331, version 11.4.0 release 11, Tech. Rep., Jun. 2013.

[16] X. Yan, N. Mani, and Y. Sekercioglu, "A traveling distance prediction based method to minimize unnecessary handovers from cellular networks to WLANs," *IEEE Commun. Lett.*, vol. 12, no. 1, pp. 14–16, 2008.

[17] D. Hong and S. Rappaport Stephen, "Traffic modeling and performance analysis for cellular mobile radio telephone systems with prioritized and nonprioritized handoff procedures," *IEEE Trans. Veh. Technol.*, vol. 35, no. 3, pp. 77–92, 1986.